

Torsional rigidity of arbitrarily shaped composite sections by hybrid finite element approach

Kutlu Darılmaz[†], Engin Orakdogen and Konuralp Girgin

Istanbul Technical University, Faculty of Civil Engineering, 34469, Istanbul, Turkey

Semih Kucukarslan

Istanbul Technical University, Faculty of Art & Letters, Department of Engineering Sciences, 34469, Istanbul, Turkey

(Received May 9, 2006, Accepted April 26, 2007)

Abstract. The purpose of this study is to calculate the torsional rigidity of arbitrarily shaped composite sections on the basis of hybrid finite element approach. An analogy is used between the torsion problem and deformation of a plate which exhibits only shear behavior. In the analysis a simple hybrid finite element based on Hellinger-Reissner functional is presented and a set of numerical examples are performed to demonstrate and assess the performance of the developed element in practical applications.

Keywords: torsional rigidity; Saint-Venant's stress function; plate; hybrid finite element.

1. Introduction

Composite cross sections are widely used in structural members in the civil and mechanical engineering applications. Therefore, a great deal of attention has been paid to develop efficient methods to calculate the properties of such sections. Continuous research efforts have been devoted in the recent years to the development of the more efficient and accurate methods.

Since many engineering structures, such as beams, shafts and airplane wings, are subjected to torsional moments, the torsional problem has been of practical importance in structural analysis. Krenk and Jeppesen (1989) studied elastic beam cross sections of moderate wall thickness in terms of finite elements with the warping function as primary variable, Savoia and Tullini (1993) investigated elastic response of inhomogeneous orthotropic beams with general cross-section and subject to uniform torsion. Ladeveze and Simmonds (1998) presented the exact beam theory for anisotropic, heterogeneous and axially piecewise constant cross sections, Swanson (1998) reviewed an existing solution for the problem of torsion of orthotropic laminated rectangular bars and then extended to the case of laminated cross-sections with high aspect ratio. Li *et al.* (2000) studied the torsional rigidity of arbitrarily shape bar made of different materials and proposed a finite element based on Galerkin's method. El Fatmi and Zenzri (2004) proposed a numerical method for the exact elastic beam theory and its applications to

[†]Assistant Professor, Corresponding Author, E-mail: kdarilmaz@ins.itu.edu.tr

homogeneous and composite beams. Kolodziej and Fraska (2005) studied the torsion of bars possessing a regular polygonal cross-section by means of boundary collocation method, Najera and Herrera (2005) presented a method to approximate the torsional rigidity of any cylindrical solid cross-section.

Obtaining the torsional rigidity of the section precisely is essential in torsion problems. The exact solutions can be found for few cross-sections such as circle, ellipse and equilateral triangle. Since the analytical solutions were limited to boundary conditions, loading and geometry, it was necessary to get the numerical solutions. Numerical methods are usually necessary for more complicated shapes. In this paper calculation of torsional rigidity of arbitrarily shaped composite sections on the basis of hybrid finite element approach is presented. Some available analytical results and numerical results from the previous studies will be compared to verify the proposed method. Finally, a hollow bridge deck and a viaduct column will be presented for complex geometries.

2. Formulation

General shape of a composite section is given in Fig. 1. Each region of the composite section is considered to be linearly elastic and isotropic. The classical solution of the displacements are given by Lekhnitskii (1963).

$$u = -\theta zy \quad (1)$$

$$v = \theta zx \quad (2)$$

$$w = \theta \psi_i(x, y) \quad (3)$$

where u , v and w are displacements in the x , y , and z directions. θ is the twist angle per unit length. $\psi_i(x, y)$ is the warping function for the i th region. The standard strain-displacement relation in terms of the warping function is given by

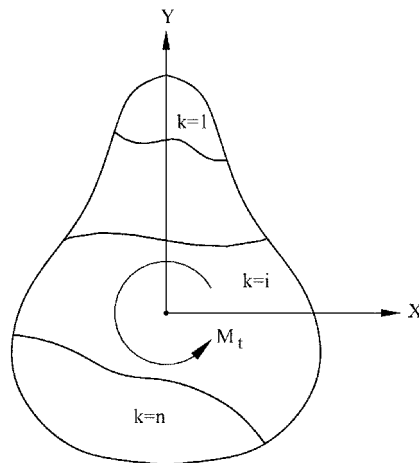


Fig. 1 General shape of the composite cross-section

$$\gamma_{xz} = \theta \left(\frac{\partial \psi_i}{\partial x} - y \right) \quad (4)$$

$$\gamma_{yz} = \theta \left(\frac{\partial \psi_i}{\partial y} + x \right) \quad (5)$$

For the stress-strain relation, following equations can be written by using Eqs. (4) and (5)

$$\tau_{xz} = G_i \theta \left(\frac{\partial \psi_i}{\partial x} - y \right) \quad (6)$$

$$\tau_{yz} = G_i \theta \left(\frac{\partial \psi_i}{\partial y} + x \right) \quad (7)$$

where G_i is the shear modulus of the i th region.

By introducing the Saint-Venant's stress function, one can write the shear stresses as:

$$\tau_{xz} = \frac{\partial \phi_i}{\partial y} \quad (8)$$

$$\tau_{yz} = \frac{\partial \phi_i}{\partial x} \quad (9)$$

where ϕ_i is called the Saint-Venant's stress function.

By taking the derivatives of the Eqs. (8) and (9) and substituting in the Eqs. (6) and (7) and then taking the differences of the Eqs. (6) and (7) gives the final partial differential equation to be solved and it is given by

$$\frac{1}{G_i} \frac{\partial^2 \phi_i}{\partial x^2} + \frac{1}{G_i} \frac{\partial^2 \phi_i}{\partial y^2} = -2\theta \quad (10)$$

There are two boundary conditions. The stress function should be continuous at each interface of the region and should be zero at the boundaries of section.

Torsional rigidity of cross-sections require the solution to the following partial differential Eq. (10).

The torsional rigidity, assuming $\theta=1$, can be obtained by

$$GJ = 2 \int_A \phi dA \quad (11)$$

Differential Eq. (10) is mathematically equal in form to the differential equation of a plate which exhibits only shear behavior. Displacements of such a plate behavior is governed by the equation

$$\frac{\partial^2 w}{\partial x^2} + \frac{\partial^2 w}{\partial y^2} = \frac{p(x, y)}{G_p} \quad (12)$$

where G_p is the shear rigidity of the plate with unit height, w is the deflection, $p(x, y)$ is the external load. The volume of the deformed plate region is recovered by

$$V = \int_A w dA \quad (13)$$

By using the analogy between Eq. (12) and Eq. (10), one can solve Eq. (12), substitute in Eq. (13) and obtain the torsional rigidity as

$$GJ = 2V \quad (14)$$

In this paper Eq. (12) is discretized by an assumed stress hybrid finite element. By using different material properties for different elements, the torsional rigidity of the arbitrarily composite sections can be easily obtained.

While using assumed stress hybrid finite element, the Hellinger-Reissner, two field variational principle in which stresses and displacements are assumed independently (Pian and Chen 1982, Gendy et al. 1992, Washizu 1982, Darilmaz 2005) is utilized. For a typical shear plate element the Hellinger-Reissner functional can be written as

$$\Pi_{RH} = \int_A \{\sigma\}^T [D] \{w\} dA - \frac{1}{2} \int_A \{\sigma\}^T [S] \{\sigma\} dA \quad (15)$$

where $\{\sigma\}$ is the independently assumed stress-resultant vector which can be conveniently written in terms of extensional plate shear forces as

$$\{\sigma\} = \{Q_x \ Q_y\}^T \quad (16)$$

where Q is the shear force; $[D]$ is the differential operator matrix, $[S]$ is the compliance matrix and A is the area of element.

$$[S] = \begin{bmatrix} 1/G_p & 0 \\ 0 & 1/G_p \end{bmatrix} \quad (17)$$

$$[D] = \begin{bmatrix} \partial/\partial x & 0 \\ 0 & \partial/\partial y \end{bmatrix} \quad (18)$$

The approximation for stress and displacements can now be incorporated in the functional. The stress field is described in the interior of the element as

$$\{\sigma\} = [P] \{\beta\} \quad (19)$$

and a compatible displacement field is described by

$$\{w\} = [N] \{q\} \quad (20)$$

where $[P]$ and $[N]$ are matrices of stress and displacement interpolation functions and $\{\beta\}$ and $\{q\}$ are the unknown stress and nodal displacement parameters, respectively. Intra-element equilibrating stresses and compatible displacements are independently interpolated. Since stresses are independent from element

to element, the stress parameters are eliminated at the element level and a conventional stiffness matrix results. This leaves only the nodal displacement parameters to be assembled into the global system of equations.

Substituting the stress and displacement approximations Eq. (19), Eq. (20) in the functional Eq. (15)

$$\Pi_{RH} = [\beta]^T[G][q] - \frac{1}{2}[\beta]^T[H][\beta] \quad (21)$$

where

$$[H] = \int_V [P]^T[S][P]dV \quad (22)$$

$$[G] = \int [P]^T[D][N]dV \quad (23)$$

Now imposing stationary conditions on the functional with respect to the stress parameters $\{\beta\}$ gives

$$[\beta] = [H]^{-1}[G][q] \quad (24)$$

Substitution of $\{\beta\}$ in Eq. (17), the functional reduces to

$$\Pi_{RH} = \frac{1}{2}[q]^T[G]^T[H]^{-1}[G][q] = \frac{1}{2}[q]^T[K][q] \quad (25)$$

where

$$[K] = [G]^T[H]^{-1}[G] \quad (26)$$

is recognized as stiffness matrix.

The plate element which exhibits only shear behavior and the nodal unknowns are depicted in Fig. 2.

The assumed stress field for the element which satisfies the equilibrium conditions for zero body forces and avoids rank deficiency is given as

$$Q_x = \beta_1 + \beta_2x + \beta_3y \quad (27a)$$

$$Q_y = \beta_4 + \beta_5x - \beta_3y \quad (27b)$$

where β_1 , β_2 and β_3 are stress parameters.

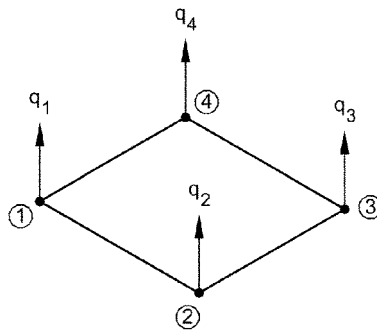


Fig. 2 Node numbering and nodal unknowns of the plate finite element

3. Numerical examples

In this section, a number of problems are examined. The results obtained are compared with analytic and some other element solutions from the literature.

3.1 Example 1

In order to check the computer program and computation accuracy, the torsional rigidity of a typical example of a hollow circular section is calculated by the proposed procedure and compared with the theoretical result. The theoretical value of the torsion constant of the hollow circular section can be obtained from the formula (Timoshenko 1968).

$$GJ = \frac{\pi D_2^4}{32} \left(1 - \left(\frac{D_1}{D_2} \right)^4 \right) \quad (28)$$

where D_1 and D_2 are inner and outer diameters of circles of the hollow circular section, respectively.

Fig. 3 shows the geometry and finite element mesh of the hollow circular section. As shown in the figure, two different mesh configurations are employed.

The numerical results are listed in Table 1. It can be seen that the results converge to the theoretical value when the finite element mesh becomes finer.

3.2 Example 2

Rectangular composite sections made of two different materials for different configurations are analyzed, Fig. 4. These cross sections are extracted from Fatmi and Zenzri (2004) which are solved by using the numerical implementation of the exact elastic beam theory and three dimensional finite elements.

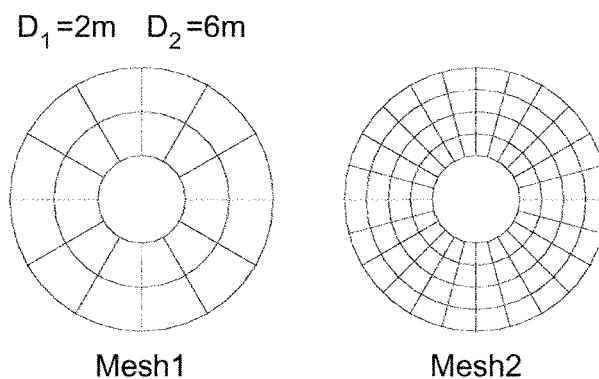


Fig. 3 Finite element meshes of hollow circular section

Table 1 Comparison of results obtained using different finite element mesh

	Mesh 1	Mesh 2	Theoretical
Torsional Rigidity GJ (kNm ²)	122.7362	124.7196	125.6637
Error (%)	2.3	0.75	---

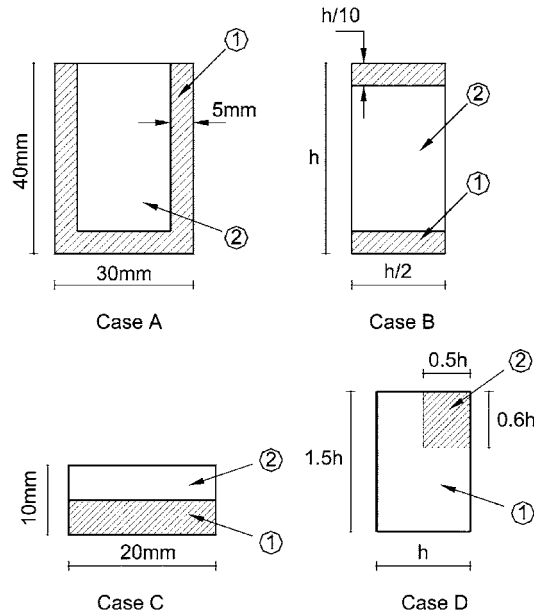


Fig. 4 Rectangular composite sections

Table 2 Comparison of the torsional rigidity ratios for different cases

Case	G_1 (GPa)	G_2 (GPa)	ν_1	ν_2	$\frac{GJ}{(GJ)_1}$ Fatmi and Zenzri (2004)	$\frac{GJ}{(GJ)_1}$ This study
A	27.51	4.02	0.33	0.33	0.5249	0.5248
B	25.00	0.345	0.00	0.45	0.0307	0.0303
C	0.345	0.500	0.45	0.45	0.8251	0.8250
D	0.455	3.846	0.10	0.30	1.5314	1.5263

In case of homogeneous material (Material 1), the analytical torsional rigidity for CASE C is available Muskhelishvili (1963), and its value is $J = 16k_1 a^3 b = 4580 \text{ mm}^4$, where $a = 5 \text{ mm}$, $b = 10 \text{ mm}$, $k_1 = 0.229$. The obtained result for homogeneous section is $J = 4561 \text{ mm}^4$, with a % 0.41 error.

Current results are compared with other solutions and given in Table 2.

It can be observed from the Table 2 that the obtained results are in a good agreement with other solutions.

The variation of ϕ function over the surface of cross-section for each case is given in Fig. 5.

3.3 Example 3

In this example a circular cross section composed of two different materials is considered, Fig. 6. The material properties for the circular section is $G_1 = 8333 \text{ MPa}$, $G_2 = 80769 \text{ MPa}$.

The calculated values of the torsional rigidity for homogenous (having material property of section 1) and the composite cross-section is given in Table 3. The variation of the stress function on the surface of the cross-section is plotted in Fig. 7.

For the circular section, the analytical solution is available and it is given by the following

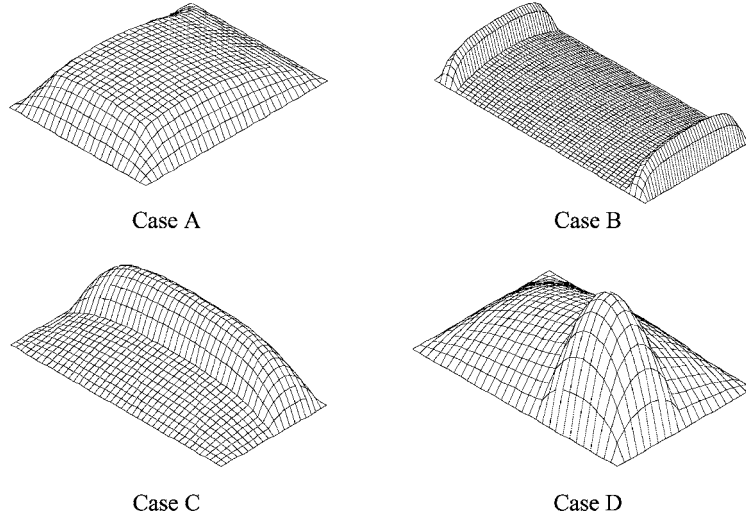


Fig. 5 Distribution of ϕ function over the surface of cross-section

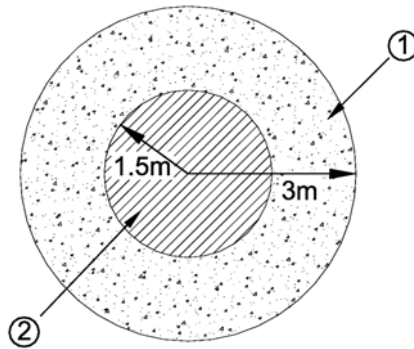


Fig. 6 Circular cross-section

Table 3 Torsional rigidity values for circular cross-section

	$(GJ)_{homogeneous}$ [MPa.m ⁴]	$GJ_{composite}$ [MPa.m ⁴]
Theoretical	1.059×10^6	1.636×10^6
This study	1.061×10^6	1.624×10^6

$$GJ = G_1J_1 + G_2J_2 \tag{29}$$

Based on the Eq. (29), the calculated value of the torsional rigidity is 1.636×10^6 MPa.m⁴ with an error of 0.71%.

3.4 Example 4: hollow bridge deck

To illustrate the generality of the proposed method, a cross section of a hollow bridge deck composed of two different materials is analyzed. The dimension and material properties are given in Fig. 8.

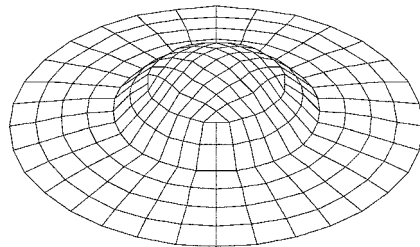


Fig. 7 3D variation of the stress function on the cross-section for circular shape

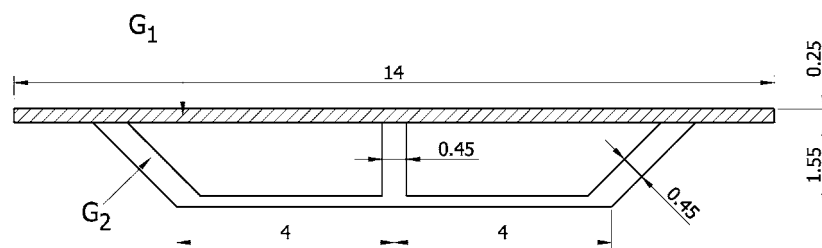


Fig. 8 Hollow bridge deck ($G_1 = 8333$ MPa, $G_2 = 14583$ MPa)

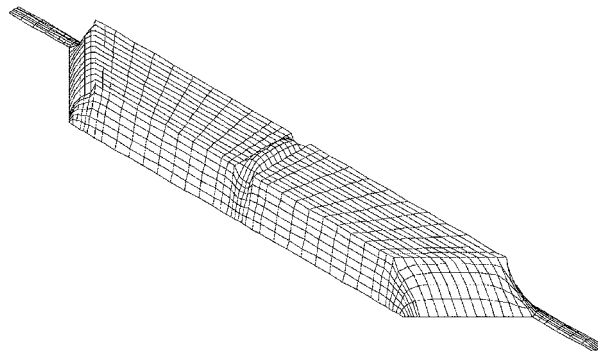


Fig. 9 3D variation of the stress function on the cross-section for bridge deck

The torsional rigidity of bridge deck is obtained as $GJ = 1.05559 \times 10^8$ MPa.m⁴ and the variation of the stress function on the surface of the cross-section is plotted in Fig. 9.

3.5 Example 5: viaduct column

Due to the requirement of finite element modeling for the strengthening project of Mecidiyekoy viaduct in Istanbul, the proposed procedure has been used to compute the torsional rigidity of the viaduct column sections, Fig. 10.

The material constants of the strengthened and existing concrete are taken as $E_1 = 32500$ MPa, $\nu_1 = 0.2$, $E_2 = 21000$ MPa, $\nu_2 = 0.2$, respectively. The torsional rigidity of this section is calculated by the proposed procedure to be $GJ = 1.12721 \times 10^8$ MPa.m⁴.

The variation of the stress function on the surface of the cross-section is plotted in Fig. 11.

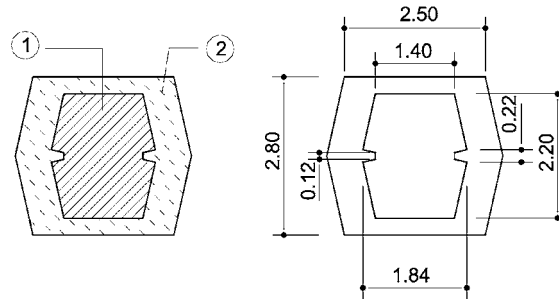


Fig. 10. Section configuration of strengthened Mecidiyekoy viaduct column

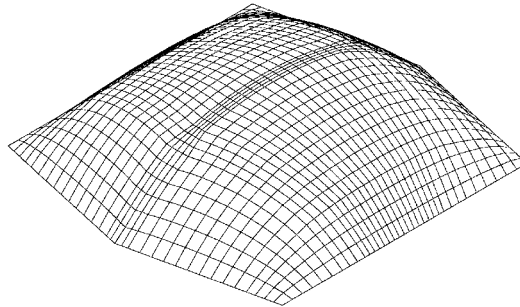


Fig. 11 3D variation of the stress function on the cross-section for the viaduct column

4. Conclusions

The torsional rigidity of the composite sections made of different material properties was analyzed on the basis of hybrid finite element procedure. In the derivation of the differential equation an analogy between the torsion problem and deformation of a shear plate problem was used. The obtained partial differential equation was discretized by hybrid finite elements to obtain the deformation in the nodal points. To test the validity of the formulations, some numerical results from the previous studies were successfully examined. It was concluded that the proposed method is simple and efficient and in a good agreement with previously published results.

References

- Darılmaz, K. (2005), "An assumed-stress finite element for static and free vibration analysis of Reissner-Mindlin plates", *Struct. Eng. Mech.*, **19**(2), 199-215.
- Darılmaz, K. (2005), "A hybrid 8-node hexahedral element for static and free vibration analysis", *Struct. Eng. Mech.*, **21**(5), 571-590.
- El Fatmi, R. and Zenzri, H. (2004), "A numerical method for the exact elastic beam theory. Applications to homogeneous and composite beams", *Int. J. Solids Struct.*, **41**, 2521-2537.
- Gendy, A.S., Saleeb, A.F. and Chang, T.Y.P. (1992), "Generalized thin-walled beam models for flexural-torsional analysis", *Comput. Struct.*, **42**(4), 531-550.
- Krenk, S. and Jeppesen, B., (1989), "Finite Elements for beam cross-sections of moderate wall thickness", *Comput. Struct.*, **32**(5), 1035-1043.

- Kolodziej, J.A. and Fraska, A. (2005), "Elastic torsion of bars possessing regular polygon in cross-section using BCM", *Comput. Struct.*, **84**, 78-91.
- Ladevèze, P. and Simmonds, J.G., (1998), "New concepts for linear beam theory with arbitrary geometry and loading", *European J. Mech., A/Solids*, **17**(3), 377-402.
- Lekhnitskii, S.T. (1963), *Theory of Elasticity an Anisotropic Elastic Body.*, Holden day, San Francisco.
- Li, Z., Ko, J.M. and Ni, Y.Q. (2000), "Torsional rigidity of reinforced concrete bars with arbitrary sectional shape", *Finite Elements in Analysis and Design*, **35**, 349-361.
- Muskhelishvili, N.I. (1963), *Some Basic Problems of the Mathematical Theory of Elasticity*, Noordho International Publishing, Leyden.
- Najera, A., Herrera, J.M. (2005), "Torsional rigidity of non-circular bars in mechanisms and machines", *Mechanism and Machine Theory*, **40**, 638-643.
- Pian, T.H.H. and Chen, D.P. (1982), "Alternative ways for formulation of hybrid stress elements", *Int. J. Numer. Meths. Eng.*, **18**, 1679-1684.
- Swanson, S.R. (1998), "Torsion of laminated rectangular rods", *Compos. Struct.*, **42**, 23-31.
- Savoia, M. and Tullini, N., (1993), "Torsional response of inhomogeneous and multilayered composite beams", *Compos. Struct.*, **25**, 587-594.
- Timoshenko, S.P. (1968), *Elements of Strength of Materials*, 5th Edition, Princeton NJ, Van Nostrand.
- Washizu, K. (1982), *Variational Method in Elasticity and Plasticity*, Pergamon Press, Oxford, 3rd. Edn.

Notation

E	: modulus of elasticity
G	: shear modulus of elasticity
GJ	: torsional rigidity
Q_x, Q_y	: internal shear force components
ν	: Poisson ratio
ϕ	: Saint-Venant's stress function
θ	: angle of twist per unit length
$[D]$: differential operator matrix
$[G]$: nodal forces corresponding to assumed stress field
$[N]$: shape functions
$[P]$: interpolation matrix for stress
$\{q\}$: displacement components
$\{w\}$: displacements
$\{\beta\}$: stress parameters
$\{\sigma\}$: internal forces

CC